

Lithium Containing Rare-Earth Metal Germanide, Er_{3.93}Li_{1.07}Ge₄: Synthesis, Crystal Structure and Chemical bonding

Gnu Nam, Beom Yong Jeon, Youngjo Kim, Sung Kwon Kang,[†] and Tae-Soo You*^{*}

Department of Chemistry, Chungbuk National University, Cheongju, Chungbuk 361-763, Korea

*E-mail: tsyou@chugbuk.ac.kr

[†]Department of Chemistry, Chungnam National University, Daejeon 305-764, Korea

Received February 7, 2013, Accepted February 28, 2013

Key Words : Polar intermetallic compound, Homogeneity-range, Electronic structure, Site-preference

The magnetocaloric effect (MCE) is known as an adiabatic change or an isothermal entropy change observed in magnetic materials when those are exposed to the external magnetic field. Since magnetic compounds displaying the giant MCE can be considered as candidate materials for the magnetic refrigeration application, the discovery of the giant MCE in Gd₅Si₂Ge₂ near room temperature in 1997 by Pecharsky and Gshneidner¹ triggered extensive worldwide investigations for the Gd₅Si₂Ge₂-related phases having a general formula of RE₅Ti₄ (RE = rare-earth metals, Ti = tetrrels) from experimental and theoretical perspectives.^{2,3} Since it has been known that the giant MCE observed in Gd₅Si₂Ge₂ originates from the reversible bond breaking and formation process of interslab Ge-Ge dimers and the corresponding magnetic characters of rare-earth metals,⁴ comprehensive substitution chemistry has been conducted *via* the cation or anion replacements in the RE₅Ti₄ family to optimize the correlation between crystal structures and magnetic properties.^{2b,3c}

During our systematic investigation for the cation substitution in the RE₄LiGe₄ (RE = early-to-mid rare-earth metals) series using the smallest monovalent element Li, we found a very narrow homogeneity-range in the Sm analogue leading to a non-stoichiometric chemical formula of Sm_{3.98(1)}Li_{1.02}Ge₄.⁵ The iso-structural compounds with a very narrow homogeneity-range were also recently reported by Suen et al. for the RE_{4-x}Li_xGe₄ (RE = Nd, Sm, and Gd; x ≈ 1.03) series.⁶ However, these recent observations are inconsistent with the previous articles by Pavlyak *et al.* (1990)⁷ and Peter *et al.* (2012)⁸ reporting only stoichiometric compositions for the RE₄LiGe₄ series. Since these recently observed homogeneity-range is confirmed only for several members including early-to-mid rare-earth metals in the RE₄LiGe₄ series and the earlier reports⁶ were mostly based on the powder X-ray diffraction data, we attempted to verify the possibility of having the homogeneity-range in the series containing the late rare-earth metals using single-crystal X-ray diffraction data. Therefore, in this work, we report synthesis, crystal structure including the disorder of Li at the rare-earth metal site and electronic structures of Er_{3.93(1)}-Li_{1.07}Ge₄.

Experimental

The stoichiometric mixture of elements (Er, Li, and Ge from Alfa Aesar; 99.9%) was added in the Nb-ampoule (*ca.* 4 cm), and both ends of the ampoule were sealed using arc-welding under the partial argon atmosphere. Then, the Nb-ampoule was sealed again in a fused-silica jacket to prevent oxidation at the elevated temperature in a tube-furnace. The reactants were heated up to 1080 °C by 200 °C/h, held there for 5 h, then cooled down to 750 °C by 5 °C/h and annealed there for 2 days. After then, the furnace was turned off, and the reactants were cooled down to room temperature naturally. The products were needle or block shape metallic silver lustered crystals and were stable for more than two months under ambient condition.

Table 1. Single-crystal crystallographic data and structure refinement result for Er_{3.93(1)}Li_{1.07}Ge₄

Crystal system	Orthorhombic
Space group	<i>Pnma</i>
Unit cell dimensions (Å)	<i>a</i> = 7.0376(4) <i>b</i> = 14.5260(7) <i>c</i> = 7.6171(4)
<i>V</i> (Å ³)	778.68(7)
<i>Z</i>	4
ρ (calcd), mg m ⁻³	8.114
μ (Mo <i>K</i> α), mm ⁻¹	56.928
Crystal size (mm ³)	0.08 × 0.06 × 0.06
θ range for data collection (°)	3.02 to 39.38
Index ranges	-12 ≤ <i>h</i> ≤ 12, -22 ≤ <i>k</i> ≤ 25, -13 ≤ <i>l</i> ≤ 13
Reflections collected	17755
Independent reflections	2388 [<i>R</i> _{int} = 0.0706]
Data / restraints / parameters	2388 / 0 / 48
Goodness-of-fit on <i>F</i> ²	1.071
Final <i>R</i> ^a indices [<i>I</i> > 2 σ ₁]	<i>R</i> ₁ = 0.0307, <i>wR</i> ₂ = 0.0586
<i>R</i> ^a indices (all data)	<i>R</i> ₁ = 0.0416, <i>wR</i> ₂ = 0.0618
Min., Max. <i>p</i> /e Å ⁻³	3.713 and -2.674

^a*R*₁ = $\sum ||F_o| - |F_c|| / \sum |F_o|$; *wR*₂ = $[\sum [w(F_o^2 - F_c^2) / \sum w(F_o^2)^2]]^{1/2}$, where *w* = $1 / [\sigma^2 F_o^2 + (A \cdot P)^2 + B \cdot P]$, and *P* = $(F_o^2 + 2F_c^2) / 3$; A and B – weight coefficients.

Table 2. Atomic coordinates, occupancy and equivalent isotropic displacement parameters (U_{eq}^a) from single-crystal structure refinement for $\text{Er}_{3.93(1)}\text{Li}_{1.07}\text{Ge}_4$

Atom	Site	Occ.	<i>x</i>	<i>y</i>	<i>z</i>	U_{eq}^a
Er1	8 <i>d</i>	1	0.01355(3)	0.597039(16)	0.18611(3)	0.00524(6)
Er2/Li1	8 <i>d</i>	0.964(2)/0.036	0.32958(3)	0.127895(15)	0.17635(3)	0.00423(7)
Li2	4 <i>c</i>	1	0.161(2)	1/4	0.521(3)	0.024(4)
Ge1	8 <i>d</i>	1	0.16781(7)	0.03633(4)	0.46548(7)	0.00580(10)
Ge2	4 <i>c</i>	1	0.01852(10)	1/4	0.08638(11)	0.00525(13)
Ge3	4 <i>c</i>	1	0.28434(10)	1/4	0.86313(10)	0.00498(13)

Table 3. Selected interatomic distances (Å) for $\text{Er}_{3.93(1)}\text{Li}_{1.07}\text{Ge}_4$

Atomic pair	Distance	Atomic pair	Distance
Er1-Li2	3.378(13)	Ge2-Ge3	2.5281(11)
	3.428(15)	Ge1-Li2	3.133(3)
Er2/Li1-Li2	3.295(17)	Ge2-Li2	2.646(16)
	3.386(15)	Ge3-Li2	2.74(2)
Ge1-Ge1	2.6400(10)		2.793(16)

Single-crystal X-ray data was collected at room temperature using Bruker SMART APEX2 CCD-based diffractometer equipped with Mo $K\alpha_1$ radiation ($\lambda = 0.71073$ Å). The selected crystal was mounted on a glass fiber, and data collection was carried out using the Bruker's APEX2 software.⁹ The structure was solved by direct method and refined to full convergence by full matrix least-squares method on F^2 using SHELXL.¹⁰ During the initial structure refinement, we observed *ca.* 3.5% of under-occupancy at the Er2 site when the site was freed from the occupancy factor. Thus, the site was refined as a mixed-site with Er and Li, and this resulted in the composition of $\text{Er}_{3.93(1)}\text{Li}_{1.07}\text{Ge}_4$. In the last refinement cycle, atomic positions were standardized using STRUCTURE TIDY.¹¹ Important crystallographic data are displayed in Tables 1-3. Crystallographic data for the structure reported here has been deposited with FIZ, Eggenstein-Leopoldshafen, Germany (Deposition No. CSD-425755).

The series of tight-binding, linear-muffin-tin-orbital (TB-LMTO) calculations¹² were carried out using the LMTO47 program.¹³ This program package exploits the atomic sphere approximation (ASA) method, in which space is filled with overlapping Wigner-Seitz (WS) atomic spheres.¹⁴ The used WS radii are listed here: Er = 1.803-1.953 Å, Li = 1.668 Å, and Ge = 1.526-1.594 Å. The basis sets included 6*s*, 6*p*, 5*d* and 5*f* orbitals for Er; 4*s*, 4*p* and 4*d* orbitals for Ge; and 2*s*, 2*p*, and 3*d* orbitals for Li. The Er 6*p*, Ge 4*d*, and Li 2*p*, 3*d* orbitals were treated by the Löwdin downfolding technique.¹⁴ The 4*f* wavefunctions of Er were treated as core functions. The *k*-space integration was conducted by the tetrahedron method¹⁵ using 216 irreducible *k*-points in the Brillouin zone,

Results and Discussion

$\text{Er}_{3.93(1)}\text{Li}_{1.07}\text{Ge}_4$ adopts the orthorhombic space group $Pnma$ (No. 62, $Z = 4$) with Pearson code *oP36* and can be

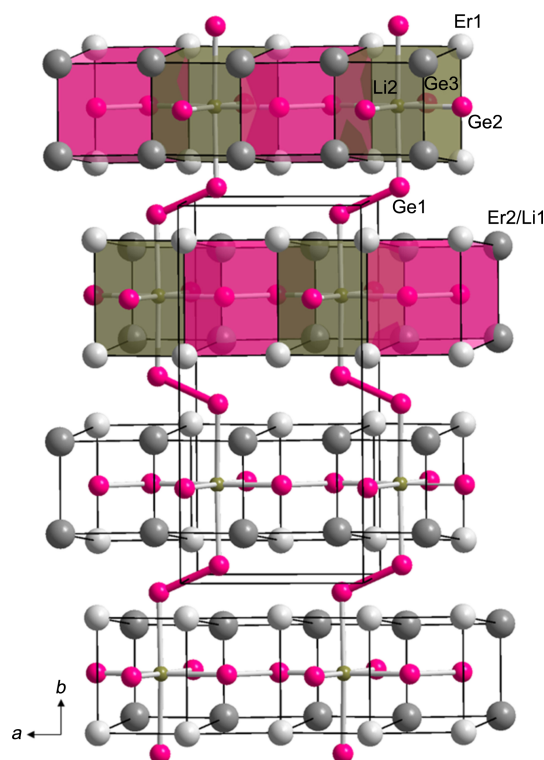


Figure 1. Crystal structure of $\text{Er}_{3.93}\text{Li}_{1.07}\text{Ge}_4$ illustrated by a combination of ball-and-stick and polyhedral representations, viewed down from the *c*-axis. A unit cell is outlined, and interslab Ge_2 dimers are highlighted in magenta-color. Color code: Er1-gray, Er2/Li1-dark gray, Ge-magenta, and Li2-gold.

considered as a ternary derivative of the RE_5Tt_4 ($RE =$ rare-earth metals; $Tt =$ tetrrels) family generated by Li substitution for rare-earth metals. There exist six crystallographically independent asymmetric atomic sites: one Er site, one mixed-site of Er and Li, one Li site, and three Ge sites.

The overall crystal structure of the title compound (Figure 1) consists of two basic structural components: 1) the 2-dimensional (2D) layered structure of the imaginary Er_2LiGe_2 slab adopting the Mo_2FeB_2 -type structure and propagating along the *ac*-plane, and 2) the dumbbell-shape interslab Ge_2 dimers located between two such neighboring Er_2LiGe_2 slabs and connecting them through the central Li in a distorted cube formed by eight Er1 and Er2/Li1 sites. In particular, each 2D Er_2LiGe_2 slabs can further be considered as a 1:1 intergrowth of the ErGe_2 and ErLi moieties adopting the AlB_2 -type and the CsCl-type structures, respectively (Figure 2).

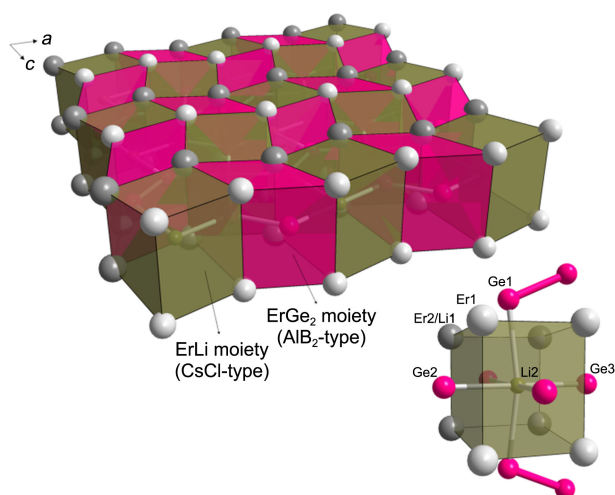


Figure 2. The 2D layered structure of an imaginary Er_2LiGe_2 slab displayed as a combined polyhedra of the ErLi and ErGe_2 moieties. The local coordination environment surrounding Li is also shown. Color code: Er1-gray, Er2/Li1-dark gray, Ge-magenta, and Li2-gold.

It has been known that the crystal structure of the RE_5Tt_4 family can be categorized in one of three major structure types,¹⁶ which are differentiated by the interatomic distance between two interslab Tt atoms: 1) for the orthorhombic Gd_5Si_4 -type structure, all interslab Tt - Tt distances fall within a single-bond dimer distance, 2) for the monoclinic $\text{Gd}_5\text{Si}_2\text{Ge}_2$ -type structure, only a half of the interslab Tt - Tt dimers are considered within a single-bond dimer distance, and 3) for the orthorhombic Sm_5Ge_4 -type structure, all interslab Tt - Tt dimers exceed the van der Waals distance ($> 3.5 \text{ \AA}$), which are considered as nonbonding. In $\text{Er}_{3.93(1)}\text{Li}_{1.07}\text{Ge}_4$, the interslab Ge_2 dimer distance is 2.64 \AA , which is considered as a single-bond, and is very well comparable to the recently reported related compounds adopting the Gd_5Si_4 -type structure: 2.58 - 2.62 \AA for $RE_{5-x}\text{Ca}_x\text{Ge}_4$ ($3.4 \leq x \leq 3.8$ for $RE = \text{La}$, $3.0 \leq x \leq 3.3$ for $RE = \text{Ce}$),¹⁷ 2.46 - 2.57 \AA for $\text{Gd}_{5-x}\text{M}_x\text{Si}_4$ ($M = \text{Zr}$, Hf ; $0.25 \leq x \leq 0.5$),¹⁸ 2.60 \AA for Yb_4MgGe_4 ,¹⁹ 2.64 - 2.70 \AA for $RE_{5-x}\text{Mg}_x\text{Ge}_4$ ($RE = \text{Gd-Tm}$, Lu , and Y),²⁰ and 2.62 - 2.63 \AA for $RE_{5-x}\text{Li}_x\text{Ge}_4$ ($RE = \text{Nd}$, Sm , Gd ; $x \approx 1.03$).⁶

In addition, the c/a ratio, which is another indicator of the formation of interslab Ge_2 dimers,^{4,16} increases up to 1.08 in title compound as comparing to 1.01 in Er_5Ge_4 (Sm_5Ge_4 -type) without the Li substitution. Therefore, $\text{Er}_{3.93(1)}\text{Li}_{1.07}\text{Ge}_4$ can be categorized in the orthorhombic Gd_5Si_4 -type structure.²¹

There exist three symmetrically independent cationic sites: the $RE1$ and $RE2$ sites occupied, respectively, by Er1 and Er2/Li1 are located on the “surface” of the 2D slabs, whereas the $RE3$ site occupied by Li2 is situated at the center of a distorted cube formed by eight $RE1$ and $RE2$ sites (Figure 2). The $RE1$ and $RE2$ sites show the total coordination numbers (CN) of 18 and 16, respectively, whereas $RE3$ site displays CN of 14. Thus, based on the local CN and interatomic distances between the central and surrounding atoms (Table 3), the volume of each cationic site can be

estimated in the following order: $RE1 > RE2 > RE3$ site.²² Interestingly, the particular site-preference is observed between Er and Li over three cationic sites: Li prefers to occupy the $RE3$ site, whereas Er prefers to be situated at the $RE1$ and $RE2$ sites. This phenomenon can surely be explained by the size-factor argument indicating that the site-preference between cationic elements was mostly governed by the cationic size rather than the electronic-factor in this case though it cannot be ignored.²²

As briefly mentioned earlier, during the initial structure refinement, we allowed the $RE2$ site be free of the occupancy factor and observed *ca.* 3.5% of under-occupancy with Er atom. Thus, we treated the $RE2$ site as a mixed-site with Er and Li, and this resulted in the final composition of $\text{Er}_{3.93(1)}\text{Li}_{1.07}\text{Ge}_4$. The Li disorder at the $RE2$ site was similar to those previously reported in the $RE_{5-x}\text{Li}_x\text{Ge}_4$ ($RE = \text{Nd}$, Sm , and Gd) series,⁶ but the amount was slightly higher with $x = 1.07$ in our compound than others with $x = 1.02$ - 1.03 . The increased Li content at the $RE2$ site can be attributed to the smaller ionic radii of Er than early-to-mid rare-earth metals ($r_{\text{Er}^{3+}} = 0.89 \text{ \AA}$ vs $r_{(\text{Nd}^{3+}-\text{Gd}^{3+})} = 0.94$ - 0.98 \AA)²³ indicating that the ionic radius of replacing elements and rare-earth metals may influence the amount of disorder or even the possibility of replacement. The similar observation related to the cationic size was also reported in the $RE_{5-x}\text{Mg}_x\text{Ge}_4$ ($RE = \text{mid-to-late rare-earth metals}$) series,²⁰ in which the series could not even be synthesized using early rare-earth metals due to the large size difference between RE and Mg. In addition, the rationale for the mixing only at the $RE2$ site rather than the $RE1$ site should be provided by the relative site-volume of cationic sites as mentioned earlier.²¹

The observed content of Li disorder in this work is not neglectful, but still quite small. Thus, in order to verify the statistical significance of our mixed-occupancy of Er and Li, we performed the Hamilton test.²⁴ The result proved that our refinement with the mixed-occupancy ($\text{Er}_{3.93(1)}\text{Li}_{1.07}\text{Ge}_4$) is better than one without the mixed-occupancy (Er_4LiGe_4). More detail procedure and result of the Hamilton test is provided in the Supporting information (Scheme S1). Therefore, we confirmed that there exists a narrow homogeneity-width in the $\text{Er}_{5-x}\text{Li}_x\text{Ge}_4$ system.

Theoretical investigations were conducted using the TM-LMTO-ASA method to study various chemical bonding and electronic structure of title compound. Due to the practical reason, calculations were carried out using an idealized composition of Er_4LiGe_4 without any mixed-site. DOS curves (Figure 3(a)) display significant valence orbital mixing among components throughout the whole energy range. In particular, the region below the Fermi level (E_F) can be divided into three sectors. The region between -10.7 and 9 eV contains major contributions from σ_s bonding interactions of interslab and intraslab Ge_2 dimers (2.640 and 2.528 \AA), and the region between -8 and -7 eV also includes major contributions of those two types of Ge_2 dimers, but from σ_s^* antibonding interactions. In addition, the region between -5 and 0 eV shows a strong orbital mixing of Er $6s$ and $5d$, and Ge $4p$ with a small contribution of Li $1s$ states. The local

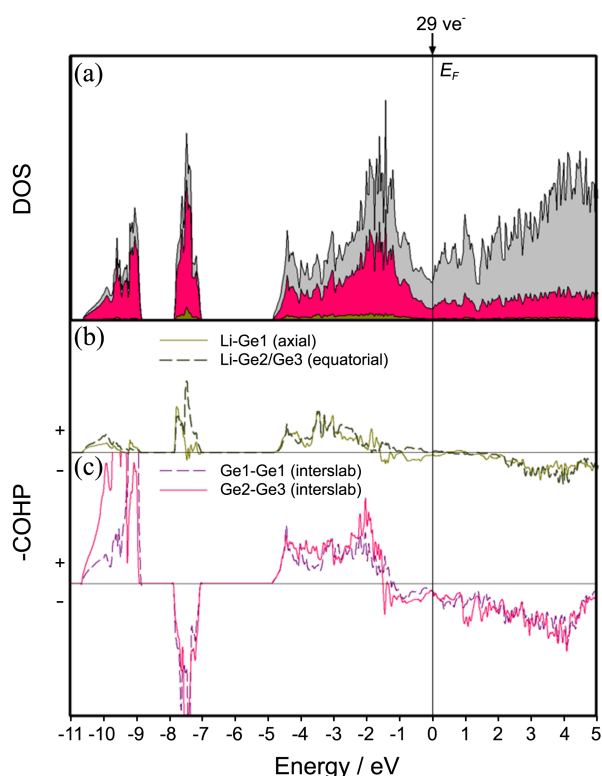


Figure 3. DOS and COHP curves of Er_4LiGe_4 . (a) Total DOS (solid black line), Er PDOS (gray-region), Ge PDOS (magenta-region), and Li PDOS (gold-region). COHP curves represent the interatomic interactions for (b) the Li-centered octahedral environment and (c) interslab and intraslab Ge_2 dimers. E_F (solid vertical line) is the energetic reference (0 eV). The region with the “+” sign represents bonding interactions, whereas the region with “-” sign represents antibonding interactions.

DOS minimum (also known as pseudogap) is observed at E_F corresponding to 29 valence electrons (ve^-) indicating the Gd_5Si_4 -type structure is energetically favorable for title compound.

Two Li-Ge COHP curves (Figure 3(b)) corresponding to interactions along either the axial- or the equatorial-direction prove two different interatomic distances of Li-Ge: the shorter Li-Ge2/Ge3 bond (2.70 Å) being nearly optimized at E_F , and the elongated Li-Ge1 bond (3.13 Å) having a weak antibonding character around E_F . COHP curves of interslab and intraslab Ge_2 dimers (Figure 3(c)) both show small unfavorable antibonding characters around E_F , but those are compensated by strong bonding characters of Er-Er interactions (Supporting information S1). These favorable interatomic interactions provide the overall structural stability. Based on the Zintl-Klemm electron counting formalism, the chemical formula of title compound can be re-written as $(\text{Er}^{3+})_{3.93}(\text{Li}^+)_{1.07}(\text{Ge}_2)^{6-}_2(0.86\text{e}^-)$ with nearly one extra valence electron, which participates in Er-Er bonding or Ge-Ge antibonding states.

Acknowledgments. This work is supported by Basic Science Research Program through the National Research Foundation of Korea (NRF) funded by the Ministry of Education, Science and Technology (grant number 2012010941) and by the research grant of the Chungbuk National University in 2010.

Supporting Information. Crystallographic data can be obtained free of charge from FIZ, D-76344, Eggenstein-Leopoldshafen, Germany, E-mail: crysdata@fiz-karlsruhe.de. The result of Hamilton test, and Er-Er COHP curves are also provided.

References

- Pecharsky, V. K.; Gschneidner, K. A., Jr. *Phys. Rev. Lett.* **1997**, *78*, 4494.
- (a) Wang, H.; Misra, S.; Wang, F.; Miller, G. J. *Inorg. Chem.* **2010**, *49*, 4586. (b) Pecharsky, V. K.; Gschneidner, K. A., Jr. *Appl. Phys. Lett.* **1997**, *70*, 3299.
- (a) Yao, J.; Wang, P.; Mozharivskiy, Y. *Chem. Mater.* **2012**, *24*, 552. (b) Yao, J.; Lyuty, P.; Mozharivskiy, Y. *Dalton Trans.* **2011**, *40*, 4275. (c) Misra, S.; Poweleit, E. T.; Miller, G. J. *Z. Anorg. Allg. Chem.* **2009**, *635*, 889.
- Choe, W.; Pecharsky, A. O.; Wörle, M.; Miller, G. J. *Inorg. Chem.* **2003**, *42*, 8223.
- Nam, G.; Jeon, J.; Kang, S. K.; Ahn, K.; You, T.-S. article in preparation.
- Suen, N. T.; You, T.-S.; Bobev, S. *Acta Crystallogr., Sect. C: Cryst. Struct. Commun.* **2013**, *C69*, 1.
- Pavlyuk, V. V.; Bodak, O. I.; Zavodnik, V. E. *Dopov Akad Nauk Ukr SSR B* **1990**, *12*, 29.
- Peter, S. C.; Disseler, S. M.; Svensson, J. N.; Carretta, P.; Graf, M. *J. J. Alloys Compd.* **2012**, *516*, 126.
- Bruker, APEX2, Bruker AXS Inc., Madison, Wisconsin, USA, 2007.
- Sheldrick, G. M., SHELXTL, University of Göttingen, Germany, 2001.
- Gelato, L. M.; Parthé, E. *J. Appl. Crystallogr.* **1987**, *20*, 139.
- (a) Andersen, O. K. *Phys. Rev.* **1975**, *B 12*, 3060. (b) Andersen, O. K.; Jepsen, O. *Phys. Rev. Lett.* **1984**, *53*, 2571. (c) Andersen, O. K. *Phys. Rev.* **1986**, *B 34*, 2439.
- Jepsen, O.; Burkhardt, A.; Andersen, O. K. The TB-LMTO-ASA Program, version 4.7, Max-Planck-Institut für Festkörperforschung, Stuttgart, Germany, 1999.
- Dronskowski, R.; Blöchl, P. E. *J. Phys. Chem.* **1993**, *97*, 8617.
- Blöchl, P. E.; Jepsen, O.; Andersen, O. K. *Phys. Rev.* **1994**, *B 49*, 16223.
- Miller, G. J. *Chem. Soc. Rev.* **2006**, *35*, 799.
- Wu, L.-M.; Kim, S.-H.; Seo, D.-K. *J. Am. Chem. Soc.* **2005**, *127*, 15682.
- Yao, J.; Mozharivskiy, Y. *Z. Anorg. Allg. Chem.* **2011**, *637*, 2039.
- Tobash, P. H.; Bobev, S. *J. Am. Chem. Soc.* **2006**, *128*, 3532.
- Tobash, P. H.; Bobev, S. *Inorg. Chem.* **2009**, *48*, 6641.22.
- Misra, S.; Miller, G. J. *J. Am. Chem. Soc.* **2008**, *130*, 13900.
- Wang, H.; Wang, F.; Jones, K.; Miller, G. J. *Inorg. Chem.* **2011**, *50* (24), p 12714.
- Shannon, R. D. *Acta Crystallogr.* **1976**, *A32*, 751.
- Hamilton, W. C. *Acta Cryst.* **1965**, *18*, 502.